

**Acting Manager:**

Dr. Mehdi Akhavan Bahabadi  
Assistant Professor  
National Center for Cyber Space

**Editor - In - Chief:**

Dr. Kambiz Badie  
Associate Professor  
ICT Research Institute

**Executive Manager:**

Dr. Ahmad Khadem-Zadeh  
Associate Professor  
ICT Research Institute

**Associate Editor (CT Section):**

Dr. Reza Faraji-Dana  
Professor  
University of Tehran

**Associate Editor (Network Section):**

Dr. S. Majid Noorhoseini  
Assistant Professor  
Amirkabir University of Technology

**Editorial Board:**

Dr. Abdolali Abdipour  
Professor  
Amirkabir University of Technology

Dr. Hassan Aghaeinia  
Associate Professor  
Amirkabir University of Technology

Dr. Vahid Ahmadi  
Professor  
Tarbiat Modares University

Dr. Abbas Asosheh  
Assistant Professor  
Tarbiat Modares University

Dr. Karim Faez  
Professor  
Amirkabir University of Technology

Dr. Hossein Gharaie  
Assistant Professor  
ICT Research Institute

Dr. Farrokh Hodjat Kashani  
Professor  
Iran University of Science & Technology

Dr. Ehsanollah Kabir  
Professor  
Tarbiat Modares University

Dr. Mahmoud Kamarei

Professor  
University of Tehran

Dr. Manouchehr Kamyab  
Associate Professor  
K. N. Toosi University of Technology

Dr. Ghasem Mirjalili  
Associate Professor  
Yazd University

Dr. Kamal Mohamed-pour  
Professor  
K.N. Toosi University of Technology

Dr. Ali Moini  
Associate Professor  
University of Tehran

Dr. Ali Movaghar Rahimabadi  
Professor  
Sharif University of Technology

Dr. Keyvan Navi  
Associate Professor  
Shahid Beheshti University

Dr. Jalil Rashed Mohasel  
Professor  
University of Tehran

Dr. Babak Sadeghian  
Associate Professor  
Amirkabir University of Technology

Dr. S. Mostafa Safavi Hemami  
Associate Professor  
Amirkabir University of Technology

Dr. Ahmad Salah  
Associate Professor  
ICT Research Institute

Dr. Hamid Soltanian-Zadeh  
Professor  
University of Tehran

Dr. Fattaneh Teghiyareh  
Assistant Professor  
University of Tehran

Dr. Mohammad Teshnehlab  
Associate Professor  
K. N. Toosi University of Technology

Dr. Mohammad Hossein Yaghmaee Moghaddam  
Associate Professor  
Ferdowsi University of Mashhad

Dr. Alireza Yari  
Assistant Professor  
ICT Research Institute

**Secretariat Organizer:**

Taha Sarhangi

**Executive Assistants:**

Valiollah Ghorbani

Nayereh Parsa-Shahla Atapour



## Topics of Interest

### Information Technology

Information Systems

IT Applications & Services

IT Platforms: Software & Hardware Technology

IT Strategies & Frameworks

### Communication Technology

Communication Devices

Communication Theory

Mobile Communications

Optical Communications

Satellite Communications

Signal / Image / Video Processing

### Network Technology

Computer & Communication Networks

Wireless Networks

Network Management

Network Security

NGN Technology

Security Management

# IJICTR

This Page intentionally left blank.

## *JNAM: a new detector proposed for marine radars*

Ali Naseri  
Department of ICT  
Imam Hussein University  
Tehran, Iran  
E-mail: anaseri@ihu.ac.ir

Jahan Jamshidi  
Department of ICT  
Imam Hussein University  
Tehran, Iran  
E-mail: Jamshidi.J62@gmail.com

Received: November 16, 2014- Accepted: May 22, 2015

**Abstract**—The proposed detector in this paper was obtained from a combination of adaptive and clutter-map detectors. Detection power of detectors has been studied in homogeneous and non-homogeneous environment (presence of interference targets) through MATLAB simulation software. The k-distribution proved to be the best option to display distribution of sea clutter, while k-distribution was assumed for sea clutter in simulation. On the other hand, CA-CFAR detector performed best in homogeneous conditions, and also the Ex-CFAR detector was suggested to improve the resistance of CA-CFAR detector against the interfering targets. The proposed detector performance was compared with these two detectors and with the ideal detector acquired from Marcum and Swerling equations, in homogeneous and non-homogeneous environment. Performance of the detectors in the presence of sharp clutter (which represents the fast clutter that make most difficult for CFAR detectors) and broad clutter (which represents the slow clutter) was investigated. Moreover, the performance of detectors in terms of data processing speed was discussed. Swerling III model for oscillating signal target was received along with the detection of a signal pulse which was also considered in all simulation.

**Key Words**-- CFAR, K-distribution, marine radar, homogeneous & non-homogeneous environment, shape parameter, false alarm

### I. INTRODUCTION

One of the main goals in automatic radar detection is to maintain the probability of false alarm constant. Finn and Johnson in [1] postulated a theory based on average math division cells of neighboring test cells, which were developed to be known as CA-CFAR detector. The CA-CFAR detector was shown to be inefficient in nonhomogeneous environment or in the presence of interfering targets. Many other techniques based on cell averaging and order statistics have been developed in the literature. Some have been discussed in [2-4]. A different approach to obtain CFAR based on clutter map exploits the intrinsic local homogeneity of the radar environment in which the detector output of each range resolution cell is averaged over several scans in order to obtain an estimate of the background level. Nitzberg in [5] developed the clutter map CFAR

processor using digital filtering to update the background power estimate corresponding to the map cell in each scan. Lops and Orsini in [6] suggested the use of a maximum selector device to provide a certain amount of protection against locally nonhomogeneous clutter. In [7], a new CFAR procedure which relied on a hybrid clutter-map strategy was introduced, with the aim of improving the system robustness against possible non-homogeneities, while preserving target detectability in a homogeneous environment. Schleher in [8] examined the detection of a steady target in Weibull clutter from a statistical detection viewpoint. Levanon et al. in [9, 10] demonstrated how to adopt Rohling's Order Statistics (OS) CFAR algorithm which was developed in [2] for a Rayleigh background, to a case of a Weibull background with known and unknown shape parameters. This paper introduced a new hybrid CFAR detector known as JNAM. This detector combines two different types of detectors,



Clutter-Map and adaptive detectors. To express more clearly the technique, the clutter-map CFAR was used in the range (spatial). This paper also described the working mechanism of the detector and then determined the appropriate values for the coefficients of the detector. Also, with the use of MATLAB simulation software, the suggested detector and CA-CFAR and Ex-CFAR detectors were simulated and the results of the simulations were compared in homogeneous situation. At the end, a loss in the suggested detector in comparison to the ideal detector which was obtained from Marcum and Swerling equations [11] was calculated in various conditions, and compared with other two detectors.

## II. ADAPTIVE AND CLUTTER-MAP DETECTORS

Suggested Detector (JNAM) in this paper is based on adaptive and Clutter-Map detectors. The following

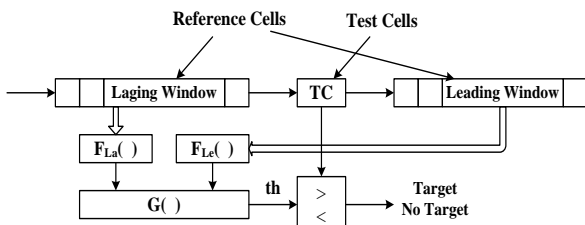


Fig.1. General Structure of adaptive CFAR detectors [13].

In this type of detector, an estimate of the threshold is obtained with  $F_{LE}(\cdot)$ ,  $F_{LA}(\cdot)$  and  $G(\cdot)$  functions, with respect to adjacent cells of the test cell. In some of the detectors, two neighbor cells of the test cell are assumed as guard cells, and so are not involved in processor computations. The reason for this is that, sometimes these cells include return signals from the target, making them not useful in the estimation of the noise power [13, 14].

## III. Clutter-Map detector (CM-CFAR)

CM-CFAR method offered to deal with nonhomogeneous Space clutter, like earth, such that, radar returns are averaged on several radar scans. However, this is not so in nonhomogeneous clutter, where it increases under clutter visibility [15, 16]. This method is most suitable when the prevalent condition favors the use of CM-CFAR, due to the reduced loss rate [17].

The CM-CFAR method, such as adaptive CFAR method scan be implement using moving-window integrator but when the number of resolution cells in Clutter-Map is high, this moving-window will require a high volume of memory, therefore CM-CFAR processors usually use a first order recursive filter to estimate the average level of interference. Figure 2 shows the block diagram of this filter [18].

section is dedicated to describe these two types of detectors.

### A. Adaptive Detectors

Figure 1 shows the general structure of an adaptive CFAR detector. This structure is same for all the CFAR detectors, with slight differences only in the functions used to obtain the threshold. Adaptive CFAR detectors can be divided into two categories: CFAR Gaussian and non-Gaussian. The Gaussian CFAR assumes a Rayleigh or exponential clutter distribution. Therefore, the only unknown parameter is power of the clutter, which should be estimated from the reference cells.

In The non-Gaussian CFARs, distribution of the clutter is assumed to be Weibull, K, log-normal or generalized Gamma, thus in addition to the power of the clutter, there are one or two other unknown parameters that must be estimated.

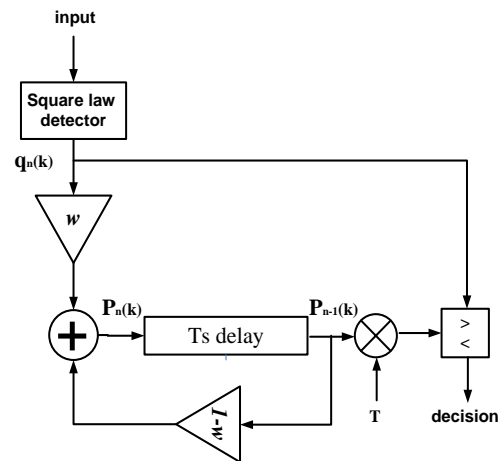


Fig. 2. Clutter map CFAR processor [17].

Using  $T$  as constant, the threshold level rises to achieve the desired false alarm rate.  $q_n(0)$  is the output of the detector in the  $n$ -th scan. The detector can be linear, logarithmic or square-low.  $T_s$  Delay is the required time for one scan of the antenna [14].

$W$ , filter coefficient, is a positive numberless that one. This parameter in CM-CFAR control filters memory (or falling time) and also is one of the determining factors of the loss in processing [14, 18]. Equation 1 describes this filter:

$$\bar{p}_n(k) = (1-w)\bar{p}_{n-1}(k) + wq_n(k) \quad (1)$$

If the square law detector is used,  $\bar{p}_n(0)$  is an estimation of interference power. In this case one can show that in the steady state, filter is equivalent with a simple CA-CFAR that uses  $N = (2-w)/w$  number of cells in estimation [14, 15, 16], with the difference that, all amounts of cells are for the same point of the radar care area obtained by the sequentially scans. This value is used to name the number of effective observations. More number of effective observations or in other words, more number of participating cells in estimation



can enhance the accuracy of clutter power estimation and thus lower processing loss.

Greater choice for  $N$  leads to smaller CFAR loss in Clutter-Map CFAR such as adaptive detectors. But on the contrary, the greater choice for  $N$  implies smaller choice for  $W$ . It means that rapid changes in the clutter should be injected slowly into the Clutter-Map (with fewer effect) and finally reducing the performance. Usually, the amount of  $N$  assumed is 15 or  $w = 0.125$ . Also  $W$  determines the falling time of the estimator. Based on falling time we can achieve the speed response of Clutter-Map for different speeds goals or clutter. So in general,  $W$  factor affects parameters or characteristics such as CM velocity, transient response of the CM and CM loss. As a result, high attention should be given in the selection of the desired value of  $W$  [14, 19].

#### IV. SUGGESTED DETECTOR (JNAM)

In this section the suggested detector was derived from adaptive and Clutter-Map detectors. Thresholding in this detector is same as Thresholding technique used in CM-CFAR. Primary output of the JNAM detector can be obtained from equation 2:

$$Y(i) = kX(i) + (1-k)Y(i-1) \quad (2)$$

Where  $k$  is a positive number smaller than one,  $X(i)$  is cell under test,  $Y(i)$  is output of the detector and  $Y(i-1)$  is previous output of the detector. The proposed Thresholding algorithm is shown in Figure 3.

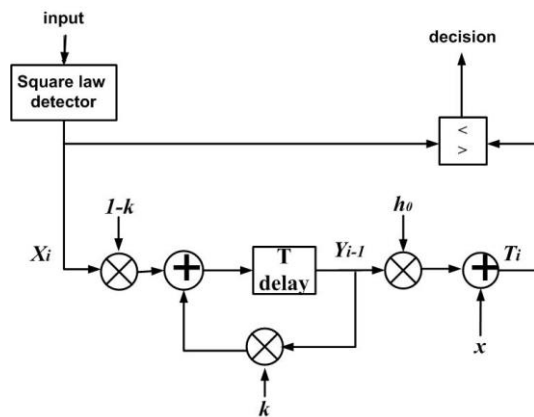


Fig. 3. Suggested algorithm for Thresholding.

After determination of the primary output of the detector, it will be multiplied by a fixed value ( $h_0$ ) which depends on the amount of  $P_{fa}$ . Then to determine the final threshold, the obtained value will be added to an additional amount ( $x$ ) which is proportion to  $P_{fa}$ . The aforementioned operations ultimately lead to the determination of the optimal threshold ( $T_i$ ). The obtained result is used to compare with the Next input value to determine the presence or absence of target in the next test cells. If the input is greater than the previously obtained threshold, it declares the presence of a target otherwise the absence of a target is declared.

#### A. Thresholding

Smaller value of shape parameter in probability density function of Weibull and k-distribution means sharper shape for distributions. Larger threshold decision is required to have a lower false alarm rate [10, 21]. Abraham in [21] presented some relationship for thresholding in different distributions. If the background of the distribution is Gaussian, assuming that the average background is  $\delta_0^2$  and assuming the probability of false alarm is  $P_{fa}$ , the threshold can be calculated as follows:

$$h = -\delta_0^2 \log P_{fa} \quad (3)$$

To normalize, this equation is divided into  $\delta_0^2$  (the average of the background) then the resultant normalized expression for threshold would be as follows:

$$\tilde{h}_0 = \frac{-\log P_{fa} \delta_0^2}{\delta_0^2} = -\log P_{fa} \quad (4)$$

It should be noted that this threshold equation is for the case of a background with Gaussian distribution. When distribution of the background is not Gaussian, this equation becomes different. In [21] threshold equations for different type of distributions including Gaussian, K and Weibull have been proposed. Table 1 presents the results

Table 1: Summary of Equations and Approximations for Detector Threshold [21].

distribution	Detector Threshold
Rayleigh/ Gaussian	$\tilde{h}_0 = -\log P_{fa}$
Weibull	$\tilde{h}_w = \frac{(-\log P_{fa})^{b-1}}{G(1+b^{-1})}$
K	$\tilde{h}_k \approx \tilde{h}_0 + \frac{a_1 \tilde{h}_0^{a_2}}{a_3 \tilde{h}_0^{0.2}}$

The purpose of this paper was to provide a detector for marine radars. Marine environment is assumed to be a Homogeneous environment with K-distribution. It has been proved that K-distribution is the most appropriate distribution to describe sea clutter [16, 22, and 23]. Therefore the proposed equation for K-distribution in [21] was used:

$$\tilde{h}_k \approx \tilde{h}_0 + \frac{a_1 \tilde{h}_0^{a_2}}{a_3 \tilde{h}_0^{0.2}} \quad (5)$$

Where  $\tilde{h}_0$  is a normalized threshold for the case of a Gaussian background distribution.  $a_1$ ,  $a_2$  and  $a_3$  are parameters that vary for different  $P_{fa}$  and selected according to Table 2. In [20] that the parameters presented in Table 2 were obtained experimentally and observed such that:

- If  $a_1 > 0$  then obtained threshold for the K-distributions will be larger than a large threshold for Rayleigh distribution. This explains the need for larger threshold due to the longer tail of the K-distribution.

- If  $a_3 > 0$  and  $V \rightarrow \infty$  then equation 5 tend to  $\tilde{h}_0$  and K-distribution will be simplified to Rayleigh distribution.

Table 2: Value of  $a_1, a_2, a_3$  parameters for different  $P_{fa}$  [21]

$P_{fa}$	$a_1$ $a_2$ $a_3$	Maximum error (dB) when $v \geq 0.2$
$10^{-2}$	0.112 2.256 0.51	0.130
$10^{-3}$	0.098 2.376 0.52	0.096
$10^{-4}$	0.128 2.245 0.51	0.070
$10^{-5}$	0.149 2.179 0.50	0.054
$10^{-6}$	0.145 2.189 0.50	0.042
$10^{-7}$	0.116 2.267 0.491	0.035
$10^{-8}$	0.234 2.018 0.481	0.032
$10^{-9}$	0.236 2.018 0.473	0.033
$10^{-10}$	0.274 1.972 0.466	0.040

In the aforementioned equation,  $v$  is shape parameter of K-distribution that can have values from  $[0.1: \infty]$ . The accuracy of the approximation over a wide range of  $v$  and  $P_{fa}$  is shown graphically in Figure 4. As shown in this curve, the approximate threshold, obtained from replacement of  $a_1$ ,  $a_2$  and  $a_3$  values in equation 5 was compared with the exact values for the different parameters. A negligible difference was observed between these two thresholds so that it can be ignored and they can be assumed to adapt together [21].

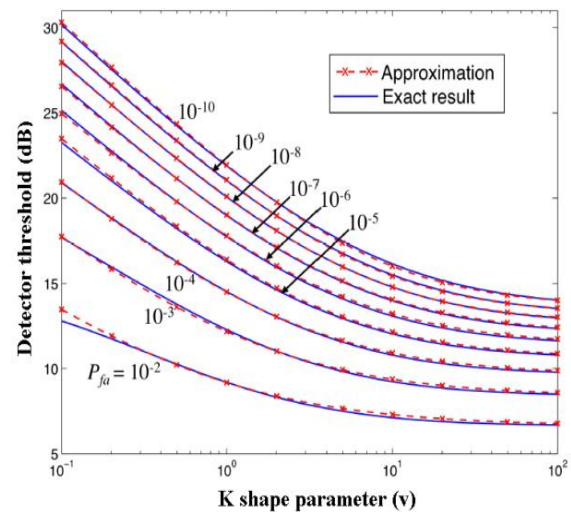


Fig. 4. Detector threshold compared with the approximation using first two rows of Table 2 [21]

The values of the parameters shown in Table 2 were obtained by minimizing the maximum error in the specified region of  $P_{fa}$  (evaluating each order of magnitude) and for  $v \in [0.2: 100]$ . The maximum error over each region as listed in the Table 2 was less than 0.2 dB. As seen in Figure 5, the error is also less than 0.2 dB when  $v \in [0.1: 0.2]$  except for  $P_{fa} = 10^{-2}$  and  $10^{-5}$  where the approximation fails below 0.2 dB. These results indicate that Equation 5 can be used with a very good approximation.

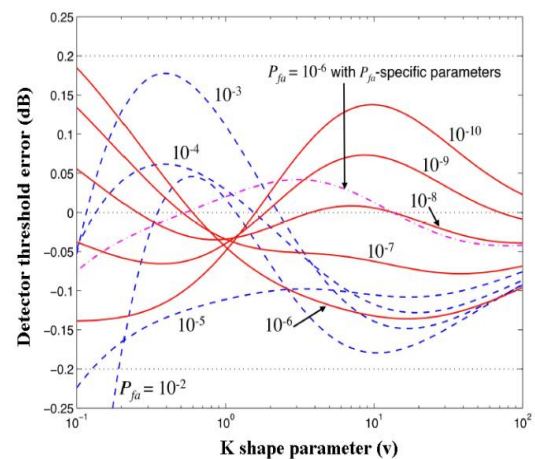


Fig. 5. Error in the detector threshold approximation for K-distributed background [21]



### B. Determining shape parameter( $v$ )for K-distribution in marine environment

From [24] the marine radars is described as follows:

$$10\text{ m} \leq h \leq 3000\text{ m} \quad (6)$$

For heights below the radar, the shape parameter ( $v$ ) of k-distribution is smaller and therefore clutter becomes spiky with longer tail. In another side, an increase in the height of radar leads to larger value for shape parameters ( $v$ ). Also in [24], Equation 7 was proposed, which showed relationship between height of radar and shape parameter of K-distribution.

$$V_{clutter} \approx \frac{1}{10} H^{\frac{2}{3}} \quad (7)$$

With replacement of equation 6 in equation 7, clearly it is seen that shape parameter of K-distribution of sea clutter should be in the range of [0.5:100].

Khalighi also stated that, for 23, in a practical situation, especially in the marine environment, shape parameters of surface clutters (including sea clutter) are in the range of [0.5:3]. Therefore with reference to [23, 24] and due to the fact that spiky clutters create main problems in Thresholding of CFAR detectors, the shape parameter were selected in the range of [0.5:5].

### C. Determining $k$ coefficient for JNAM detector

An increase in  $k$  coefficient, in the presence of interference targets or small targets near the larger goals, arising from the test cell having smaller effect in Thresholding, will result in a slow change and consequently an increase in the result probability of detection of interference targets and smaller targets closer to the larger targets. On the other hand, if the power of background is change basically or in the presence of edge clutter, whatever the amount of  $k$ , whether it becomes smaller (because the test cell will have a greater effect on Thresholding with coefficient of  $1-k$ ), the threshold will be updated with a higher speed. Therefore in selecting an optimum value for  $k$ , a compromise between the higher probability of detection (with larger  $k$ ) and faster adaption of threshold with power of background (with smaller  $k$ ) is necessary. Figure 6 shows a general view of variation of  $P_d$  versus  $k$  coefficient for different values of  $P_{fa}$ . It shows that whenever the  $k$  coefficient is closer to one,  $P_d$  becomes greater. Also in Figure 7, changes of  $P_d$  according to  $k$  coefficient are displayed on closer view. It is seen that for  $k \geq 0.99$ , power detection is reduced. This implies that the maximum amount that can be considered for  $k$  is 0.99. In these simulations, the parameter values are chosen randomly from the range of [0.5: 5]. Generally, it can be concluded that, depending on the operation environment,  $k$  coefficient should be considered greater than 0.9 and less than 0.99.

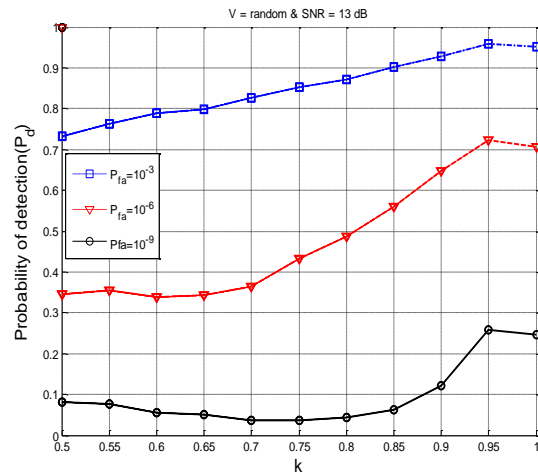


Fig. 6. Probability of detection versus  $k$  coefficient for JNAM detector (General view)

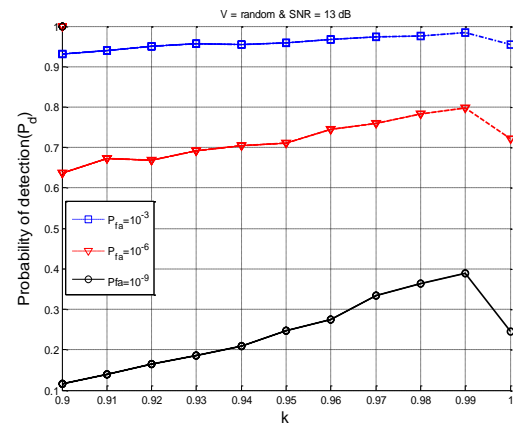


Fig. 7. Probability of detection versus  $k$  coefficient for JNAM detector (close view)

## V. EVALUATION OF JNAMDETECTOR

This section investigated the detection power in homogeneous environment, loss and speed of JNAM detector and compared the results with CA-CFAR and Ex-CFAR detectors.

### A. detection Power

This section focused on the detection power of JNAM detector and compared its results with other detectors. The detection power of JNAM for different value of  $k$  was first discussed, Followed by detection power of JNAM for different value of  $k$  compared with other detectors, with random shape parameter. It is important to note that all figures were obtained from the processing of  $10^{-6}$  cells.

#### A.1. detection power of JNAM detector for various value of $k$ coefficient

In This section detection power of JNAM detector for different values of  $k$  were discussed and the results compared with the ideal detector obtained from Marcum and Swerling equations. For this purpose, performance of detector for three values of  $k$  (0.9, 0.95, 0.99) and  $P_{fa}=10^{-6}$  is shown in Figure 8. In these





simulations the shape parameters were randomly selected from the range of  $[0.5:5]$ . As clearly seen from the figure, larger value for  $k$  (or smaller effect of input on threshold) leads to larger amount of detection power, and the performance of the detector is closer to the ideal detector. Also, in Figure 9 shows the detection power of JNAM detector for  $k=0.99$  compared to Ex-CFAR, CA-CFAR and ideal detector. This figure shows  $k=0.99$  as optimum value too.

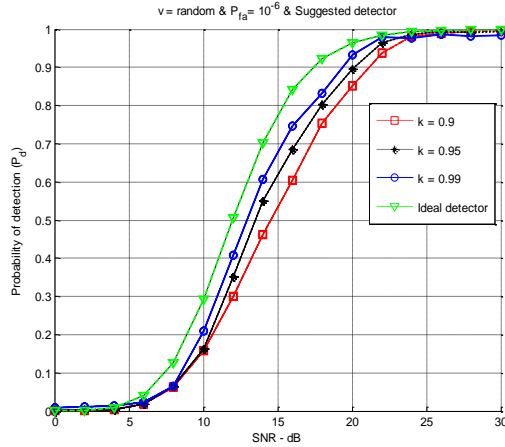


Fig. 8. Probability of detection versus SNR for JNAM detector for different value of  $k$  ( $P_{fa}=10^{-6}$ )

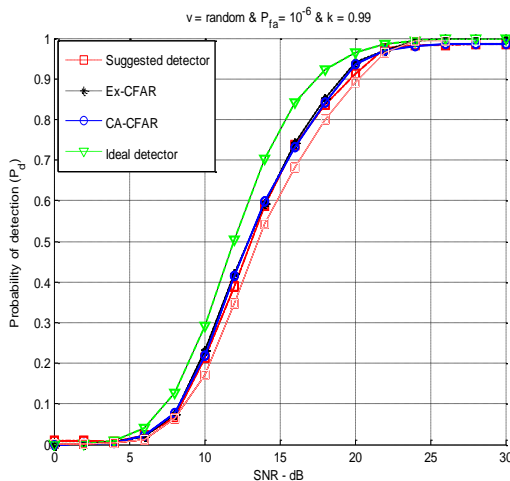


Fig. 9. Probability of detection versus SNR for different detectors

### A.2. detection Power versus SNR (different shape parameters)

This section focused on comparison of detection power of JNAM detector and other detectors for different values of shape parameter of K-distribution (0.1, 0.5, and 5). In these simulations, the  $k$  coefficient was assumed to be 0.99 and the results are shown in Figures 10 to 12. Also, in these simulations  $P_{fa}=10^{-6}$  was assumed. As seen in these curves, an increase in the  $v$  parameter resulted in JNAM detector results to become closer to the ideal detector. For example in  $v=5$ , performance of the JNAM detector will be very close to ideal detector; because in this situation clutter is not spiky and  $k$ -distribution tend to Rayleigh distribution (Figure 12).

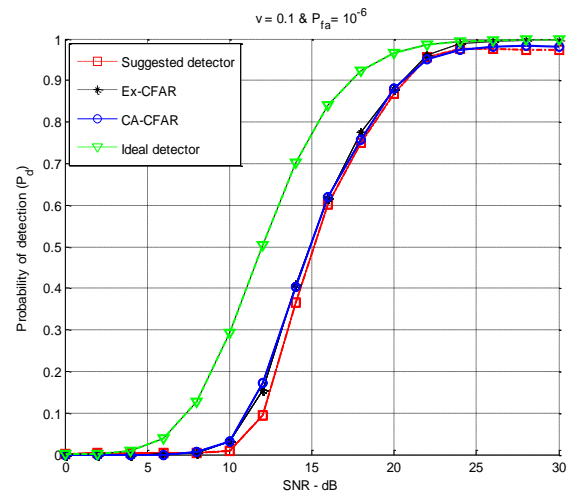


Fig. 10. Comparison Probability of JNAM detection with different detectors ( $v=0.1$ )

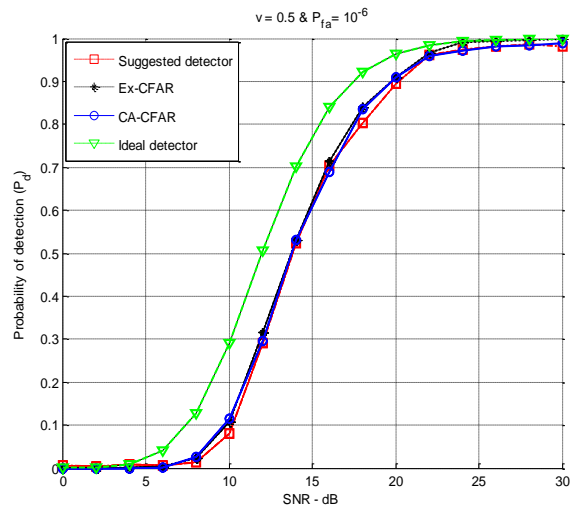


Fig. 11. Comparison Probability of JNAM detection with different detectors ( $v=0.5$ )

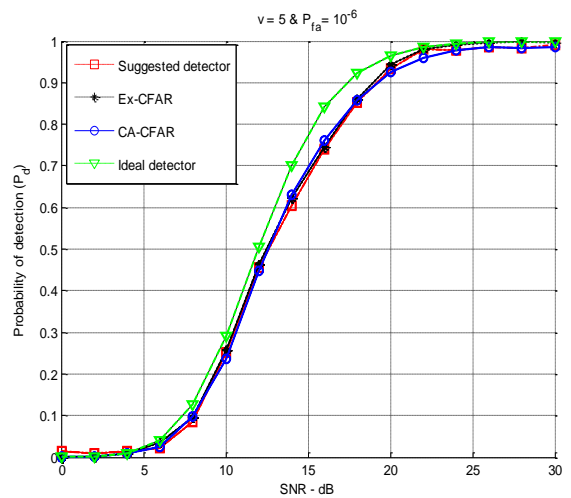


Fig. 12. Comparison Probability of JNAM detection with different detectors ( $v=5$ )

### B. Loss of detection

An important topic in the CFAR detectors is the amount of loss. If a CFAR detector is compared with



an ideal detector with known parameters, it can be observed that In a CFAR detector, due to uncertainty about clutter power, threshold level should be assumed a bit higher in order to achieve equal  $P_{fa}$  with ideal detector. This increases in threshold of CFAR detector makes the need for more signal to clutter (or noise) ratio in same probability of detection essential. The difference between needed amounts of signal to noise ratio in achieving the same  $P_{fa}$  is called CFAR loss. Obviously, better detector has smaller loss in the same situations [12, 24]. The value of  $P_d$  in which power of the detectors obtain a loss was considered at 0.5 [25, 26]. Therefore, from Figure 15, the probability of detection versus signal to noise ratio started from 0.5 for different detectors in order to obtain loss with more degree of accuracy. Figures 13 and 14 illustrates the loss of detection versus  $k$  coefficient for JNAM detector in both a general and close view. A scan be seen,  $k$  coefficient values of 0.9, 0.95 and 0.99 resulted in loss of JNAM detector values of 2.7, 1.7 and 1.1 dB, respectively. Thus the minimum loss of detection was obtained for  $k = 0.99$ , this means that the most appropriate value for  $k$  coefficient is 0.99.

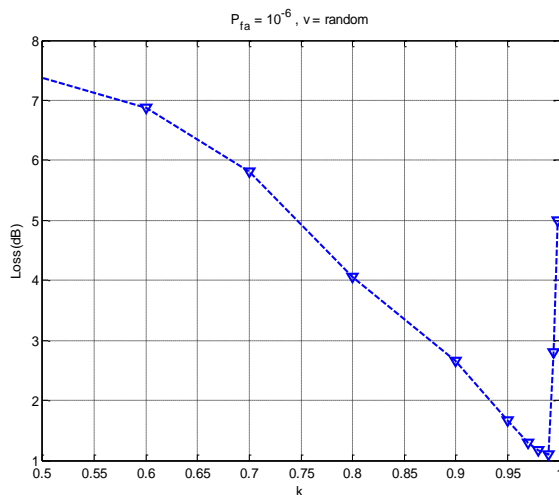


Fig. 13. Loss of detection versus  $k$  coefficient of JNAM detector (general view)

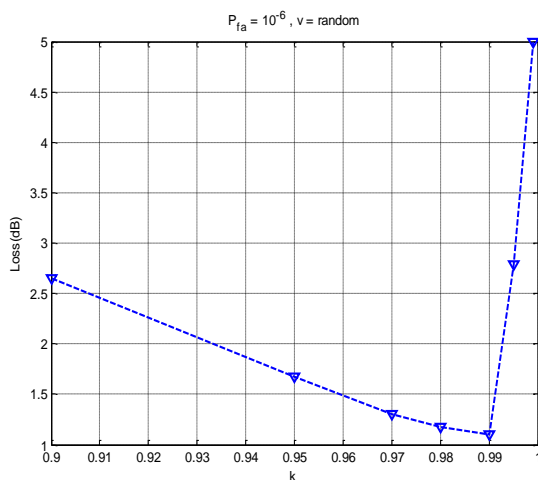


Fig. 14. Probability of detection versus  $k$  coefficient of JNAM detector (close view)

Figure 15 shows the probability of detection versus signal to noise ratio for different detectors (JNAM, CA-CFAR, Ex-CFAR and ideal detectors) in closed view to obtain loss. As shown in the figure, the performance of detectors for  $\text{SNR} \leq 22$  dB are very close together, therefore it can be said that they have similar performance. But in large amounts of signal to noise ratio ( $\text{SNR} \geq 22$  dB); Ex-CFAR a higher probability of detection than the JNAM and CA-CFAR detectors (close to optimum) was observed, because in high signal to noise ratio, clutters (especially sharp clutters) increased with the same signal to noise ratio. This resulted in the proportional increase in threshold of CA-CFAR and JNAM detectors, which reduced their detection power. But in Ex-CFAR detector the strong signals were cut off before Thresholding, resulting in a fewer increases in threshold than the other two detectors. The consequence of this is an increase in the detection power of this detector in high signal to noise ratio in comparison with the other two detectors. So its performance adapted to the ideal detector in  $\text{SNR} \geq 22$  dB. Generally, it can be concluded that the performance of each detector is same in  $\text{SNR} \leq 22$  dB but in  $\text{SNR} \geq 22$  dB the Ex-CFAR detector has better performance.

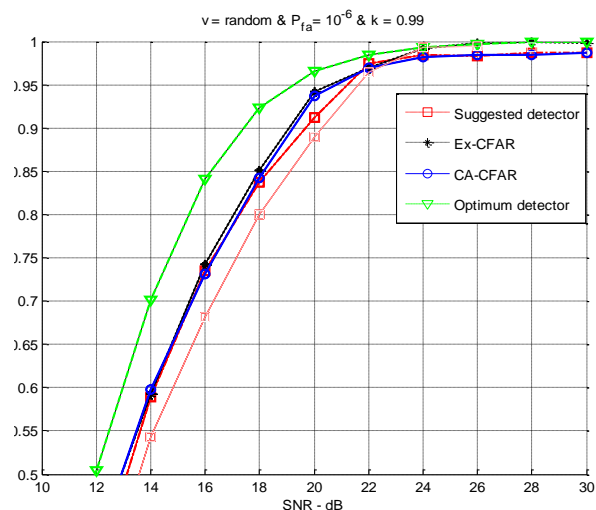


Fig. 15. Loss of detection for different detectors

It is seen In Figure 15 that the loss experienced in all the detectors was approximately equal to 1 dB. In this simulation, value of 0.99 was considered for  $k$  coefficient of the JNAM detector.

Figure 16 shows the detection loss of JNAM detector versus shape parameter of K-distribution. As seen, maximum loss was obtained for smallest shape parameter ( $v=0.1$ ). But when increase  $v$ , K-distribution tended to Rayleigh and its sharpness reduced. It leads to rising  $P_d$  and falling  $P_{fa}$ . Because detection loss of JNAM detector is similar to Ex-CFAR and CA-CFAR (from Figure 10, 11, 12) this curve can be distributed for two other detectors.

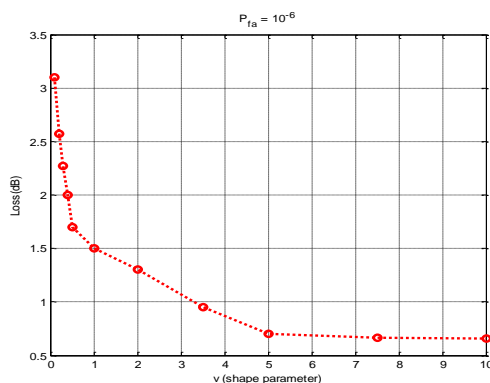


Fig. 16. Loss of detection versus shape parameter(v) for JNAM detector

### C. COMPARE THE SPEED PERFORMANCE OF DETECTORS

In This section, speed detection of detectors was compared. For this purpose, the time required in processing of 2000 pulse for different processor was compared. To ensure the results, processing time preprocessor for 500 times was tested. Briefly, 10 samples of obtained results from these tests are shown in Table 3. The obtained data has shown that required time for processing of the 2000 pulse with JNAM detector is 55% that of the required times for CA-CFAR processor and 45% that of the required times for the Ex-CFAR processor, implying a higher speed of CA-CFAR processor in comparison with Ex-CFAR (despite the fact that the number of contributed pulses in thresholding). Unlike CA-CFAR processors, before averaging of reference cells, excision process takes place, and this requires some more time. This result in the Ex-CFAR processor becoming slower than the CA-CFAR processor. These results demonstrate the high speed of JNAM processor. In fact the main advantage of this processor is its high speed. It can be said that the processing speed of JNAM processor is 2.2 and 1.8 times more than Ex-CFAR and CA-CFAR processors, respectively. It is an important advantage for this processor, because in real-time applications where rapid detection is required, speed of the processors is the most important advantage.

Table 3. Needed time for processing of 2000 pulse using different detectors.

No.	JNAM (second)	Ex- FAR (second)	CA-FAR (second)
1	0.001572	0.003494	0.002841
2	0.001610	0.003345	0.002730
3	0.001563	0.003401	0.002821
4	0.001554	0.003447	0.002969
5	0.001547	0.003484	0.002818
6	0.001562	0.003277	0.003183
7	0.001500	0.003962	0.002867
8	0.001558	0.003348	0.002847
9	0.001503	0.003268	0.002824
10	0.001555	0.003513	0.002924

### VI. CONCLUSION

In this paper a suggested detector named JNAM and ideal detectors CA-CFAR, Ex-CFAR were simulated by MATLAB software to evaluate and compare their performance. After comparing the obtained results from the simulations it was concluded that by selecting optimum value for k coefficient, performance of the JNAM detector was the same as CA-CFAR and Ex-CFAR detectors which are optimum in homogeneous conditions. Also, it was seen that a loss of JNAM detector can be only 1dB. The simulation was continuous and the speed of the detectors was discussed. The results of these simulations have shown that the speed of data processing by the JNAM detector was approximately 2.22 and 1.8 times faster than Ex-CFAR and CA-CFAR, respectively. It can be considered as the most important advantage of this detector because in real-time radar detectors, speed of detection is the most important parameter. Another advantage of JNAM detector is its simple structure and algorithm which can be easily implemented.

### REFERENCES

- [1] Finn, M. M.; Johnson, R. S.; "Adaptive Detection Mode with Threshold Control as a Function of Spatially Sampled Clutter Level Estimates", RCA Rev. 30, pp. 414-465, 1968.
- [2] Rohling, H.; "Radar CFAR Thresholding in Clutter and Multiple Target Situations", IEEE Trans. on AES, Vol. 19, No. 4, pp. 608-621, July 1983.
- [3] Hansen, V.G.; J.H. Sawyers; "Detectability Loss Due to the Greatest of Selection in a Cell Averaging CFAR", IEEE Trans. Aerospace Electron. Systems AES-16, pp. 115-118, January 1980.
- [4] Trunk G.V.; "Range Resolution of Targets Using Automatic Detectors", IEEE Trans. Aerospace Electron, Systems AES-14, pp. 750-755 September 1978.
- [5] Nitzberg, R.; "Clutter Map CFAR Analysis", IEEE AES, Vol. 22, No. 4, pp. 419-421, July 1986.
- [6] Lops, M.; Orsini, M.; "Scan-by-scan averaging CFAR", IEE Proc. Pt. F. 136 (6) 249-254, December 1989.
- [7] Lops M.; "Hybrid Clutter-Map/L-CFAR Procedure for Clutter Rejection in Non homogeneous Environment", IEE Proc. Radar, Sonar Navigation, Vol. 143, pp. 239-245 August 1996.
- [8] Schleher, D.C.; "Radar Detection in Weibull Clutter", IEEE Trans. Aerospace Electron. Systems, AES-12, pp. 736-743, November 1976.
- [9] Levanon, N.; Shor, M.; "Order statistics CFAR for Weibull background", IEE Proc. Pt. F 137 (3), pp. 157-162, June 1990.
- [10] Ravid, R.; Levanon, N.; "Maximum-likelihood CFAR for Weibull background", Radar and Signal Processing, IEE Proceedings F Volume 139, Issue 3, pp. 256 - 264, June 1992.
- [11] Skolnik, M. I.; "Introduction to Radar Systems", McGraw-Hill, 3rd Edition, 2000.
- [12] Farrouki, A.; Barkat, M.; "Automatic Censoring CFAR Detector Based on Ordered Data Variability for Nonhomogeneous Environments", IEE Proceedings Radar, Sonar Navig, Vol. 152, No. 1, pp. 43-51, Feb. 2005.
- [13] Dr noruzi, yaser, phd thesis communication / two-dimensional detectors with a fixed rate of false alarm/ sharif university
- [14] Skolnik, M. I.; "Radar Handbook", 2nd Edition, McGraw-Hill, 1990.
- [15] Hoyle, J.S.; Khoury, E.N.; "Clutter Maps: Design and Performance", IEEE, 1984.



- [16] Scheleher, D. C; "MTI and Pulsed Doppler Radar", Norwood, Artech House, 1rd Edition, 1991.
- [17] Hamadouche, M.; Barakat, M.; Khodja, M.; "Analysis of the Clutter Map CFAR in Weibull Clutter", Signal Processing, V.80, No.1, p.117-123, Jan 2000.
- [18] Farina, A. ; Studer, F. A.; "A review of CFAR detection techniques in radar systems" Microwave Journal, Vol. 29, no. 9, pp. 115-128, Sep. 1986.
- [19] Zaimbashi, A.; Nayeibi, M.M.; Taban, M.R.; "Survey of the Two Parametric CFAR Detector in Practical Scenarios", Proc. of 15th Iranian Conference on Electrical Engineering, ICEE 2007, Iran Telecommunication Research Center, Tehran, Iran, pp.100-105 ,May 16-18, 2007.
- [20] Watts, S.; "Radar Detection Prediction in Sea Clutter Using the Compound K-Distribution Model", IEE Proceedings-F, Vol. 132, pp. 613-619, December 1985.
- [21] Abraham, D. A.; "Detection-Threshold Approximation for Non-Gaussian Backgrounds", Published in IEEE Journal of Oceanic Engineering, Vol. 35, No. 2, April 2010.
- [22] Gandhi, P. P; Kassam, S. A.; "Analysis of CFAR Processors in Homogeneous Background", IEEE Trans. On AES, Vol. 24, No. 4, pp. 427-445, July 1988
- [23] Khalighy, mohammad ali, master thesis, design a receiver with constant false alarm rate for use in electronics ware /sharif university/ 1386
- [24] Denny, W.M.; "K-distributed Sea Clutter: Small Target Processing", IEE International Conference Radar-97, IEE Publication, No. 449 ,pp. 591 -595. , 14-16 October 1997.
- [25] Amanipure, vahideh, master thesis/ distributed radar detection of targets / Tehran university
- [26] Anastassopoulos, V.; Lampropoulos, G.A.; "A New and Robust CFAR Detection Algorithm", IEEE Trans on Aerospace and Electronic Systems ,Vol. 28, No. 2, pp. 420-427, April 1992.



**Ali Naseri** received the Ph.D. degree in Electronic Engineering from the Iran University of Science and Technology in 2003. He is currently an Associate Professor in the ICT department at Imam Hussein University, and has written 12 books in the field of ICT. He has also published 90 scientific papers in the related journals and conferences.



**Jahan Jamshidi** received the M.Sc. degree in electronic engineering from the University of Imam Hussein. He has published 4 scientific papers in journals and conferences. He is now working on Telecommunications Company in Tehran.





# IJICTR

This Page intentionally left blank.

